

Correlations between Pulsed X-ray Flux and Radio Arrival Time in the Vela Pulsar

A. Lommen¹, J. Donovan^{1,2}, C. Gwinn³, Z. Arzoumanian^{4,5}, A. Harding⁴, M. Strickman⁶, R. Dodson⁷, P. McCulloch⁸, and D. Moffett⁹

¹ Department of Physics and Astronomy, Franklin and Marshall College, Lancaster, Pennsylvania

² Department of Astronomy, Columbia University, New York, New York

³ Department of Physics, University of California, Santa Barbara, California

⁴ NASA Goddard Space Flight Center, Greenbelt, Maryland

⁵ Universities Space Research Association

⁶ Code 7651.2, Naval Research Laboratory, Washington, DC

⁷ Observatorio Astronómico Nacional, Madrid, España

⁸ University of Tasmania, Tasmania, Australia

⁹ Furman University, Greenville, South Carolina

Abstract. We report the results of simultaneous observations of the Vela pulsar in X-rays and radio from the RXTE satellite and the Mount Pleasant Radio Observatory in Tasmania. We sought correlations between the Vela’s X-ray and radio flux densities and radio arrival times on a pulse by pulse basis. We found significantly higher flux density in Vela’s main X-ray peak during radio pulses that arrived early. This excess flux shifts to the ‘trough’ following the 2nd X-ray peak during radio pulses that arrive later. We suggest that the mechanism producing the radio pulses is intimately connected to the mechanism producing X-rays. Current models using resonant absorption in the outer magnetosphere as a cause of the radio emission, and less directly of the X-ray emission, are explored as a possible explanation for the correlation.

1. Introduction

The complexity of Vela’s spectrum allows for the possibility of both polar cap (Daugherty & Harding 1996) and outer-gap (Cheng, Ruderman, & Zhang 2000) models of emission, but only a subset of the models suggest a connection between the radio and X-ray emission. For example Harding et al.(2002) suggest that scattering of soft X-ray photons in a polar cap model could explain the observed optical spectrum of Vela and also provide for the alignment of the radio peak with a very soft X-ray peak, which they observe. The connection between X-ray and radio emission that we offer in this article favors models such as this, which connect far reaching ends of the electromagnetic spectrum.

Additional experiments linking pulsar emission in the radio and X-ray regimes have been performed by Cusumano et al. (2003) and Vivekanand (2001).

Cusumano et al. show that in PSR B1937+21 there is close phase alignment between X-ray pulses and giant radio pulses, suggesting a correlation in their emission regions. The work by Vivekanand, on the other hand, explains the connection between the Crab pulsar’s radio and X-ray flux variations as a result of temporal variations in the number of “basic emitters” or in the basic emitters’ degree of coherence.

Giant radio pulses have not been shown to exist in Vela, but Johnston et al. (2001, hereafter J01) discovered ‘giant micropulses’ in the Vela pulsar, which have flux densities no more than ten times the mean flux density and have a typical pulse width of $\sim 400\mu s$. These micropulses may explain the results of Krishnamohan & Downs (1983, hereafter KD83) who found that the strongest radio pulses arrive earlier than the averaged profile.

By doing a pulse-by-pulse analysis of the Vela pulsar in X-ray and radio wavelengths, we will show in this paper that the emission mechanisms creating the Vela pulsar’s X-ray and radio flux densities must be related. We will discuss the X-ray and radio observations in §2, our analysis in §3, the effects of scintillation in §4, a discussion of interpretations in §5, theoretical predictions as they relate to our results in §6, and finally our conclusions and related future work in §7.

2. Observations

Our data consist of 74 hours of simultaneous radio and X-ray observations taken over three months at the Mount Pleasant Radio Observatory in Tasmania and with the RXTE satellite.

The radio data were acquired during 12 separate observations using the 26m antenna at a frequency of 990.025 MHz between 30 April and 23 August, 1998. All individual pulses from Vela are detectable, and the pulse height,

integrated area, and central time of arrival (for the solar-system barycenter) were calculated from cross-correlation with a high signal to noise template in the usual fashion.

The X-ray data were taken during the same three months, yielding 265 ks of usable simultaneous observation. For the purposes of this project, only top-layer data from RXTE’s Proportional Counter Units (PCUs) in Good Xenon mode in the energy range of 2-16 keV were used. Other filtering parameters included were standard RXTE criteria: elevation was greater than 10 degrees, offset was less than 0.02 degrees, the data were taken with at least 3 PCUs on, time since SAA was at least 30 minutes, and electron0 was less than 0.105.

3. Analysis

We filtered the X-ray photon arrival times and transformed them to the Solar System Barycenter (SSB) using the standard FTOOLS (Blackburn 1995) package. We calculated the pulsar phase at the time of each X-ray photon, and matched each X-ray photon with the radio pulse that arrived at the SSB at the same time. We then compared pulse profiles for X-rays segregated according to the arrival time of the radio pulse.

We filtered the X-ray photon arrival times and transformed them to the Solar System Barycenter (SSB) using the standard FTOOLS (Blackburn 1995) package. We calculated the pulsar phase at the time of each X-ray photon, using the radio pulsar-timing program TEMPO¹, and the ephemeris downloadable from Princeton University¹. We matched each X-ray photon with the radio pulse that arrived at the SSB during the same turn of the pulsar. The precise period of time associated with each radio pulse was given by our best model for the pulse arrival time, $\pm 0.5 \times$ the instantaneous pulse period calculated via the model. Photons arriving on the borderline were associated with the earlier pulse. We then compared pulse profiles for X-rays segregated according to the corresponding radio pulse arrival time.

Radio pulses arrive at a range of times around the predicted arrival time, as KD83 found. The histogram of residual arrival times for radio pulses, relative to the prediction of our best model, is shown in Figure 1. We divided all of the pulses into four quartiles, by the residual phase of the radio pulse, with equal numbers of pulses in each quartile. Figure 1 shows our division of the residual phase of the radio pulse into the quartiles. We called the quartiles early, medium-early, medium-late, and late, according to the arrival time of the radio pulse.

We formed an X-ray pulse profile for each of the quartiles of radio-pulse arrival times, from the X-ray photons associated with each. Figure 2 shows the four resulting X-ray profiles with errors determined by counting statistics. The X-ray profiles are significantly different; the pulse

changes in shape among the quartiles. In particular it appears that the first X-ray pulse is sharper and stronger during “early” radio pulses. Also, it appears that the trough after the 2nd X-ray peak around phase 0.4 (hereafter called simply ‘the trough’) gets “filled in” in late quartiles.

In order to graphically analyze the changes in pulse shape, we plot the profiles in different quartiles against one another in Figure 3. The solid diagonal line shows where the points would lie if the profiles were identical. As the figure shows, Bin 2 (the tallest bin in the 1st X-ray peak) is significantly stronger in the early quartile than in the late quartile. In addition, although less noticeable, Bins 12, 13 and 1 (the trough) are significantly weaker in the early quartile than in the late.

Overall, the data suggest that sharper X-ray pulses are associated with earlier radio pulses. In Figure 4 we plot the height of the peak in Bin 2, and of the trough in Bins 12 and 13, against the lateness of the quartile. The figure shows a systematic trend of a weaker peak toward late arrivals. The increase in photon rate in the trough makes up for much of the loss of X-ray photons in the peak.

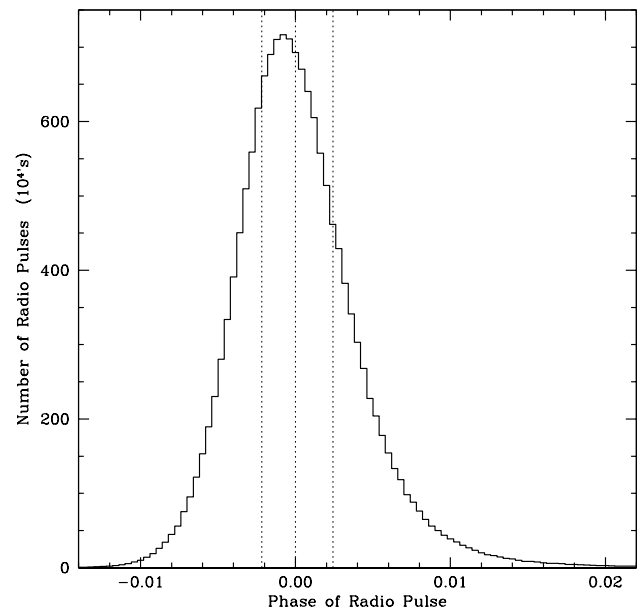


Fig. 1. The total number of radio pulses vs phase relative to a predictive long-term timing model. The dotted lines show the boundaries of the four bins that were used to make the four profiles shown in Figure 2.

4. Scintillation

In contrast to effects intrinsic to the pulsar, scintillation is unlikely to produce the observed association, because it does not affect X-rays; scintillation might erase such

¹ See <http://pulsar.princeton.edu/tempo>

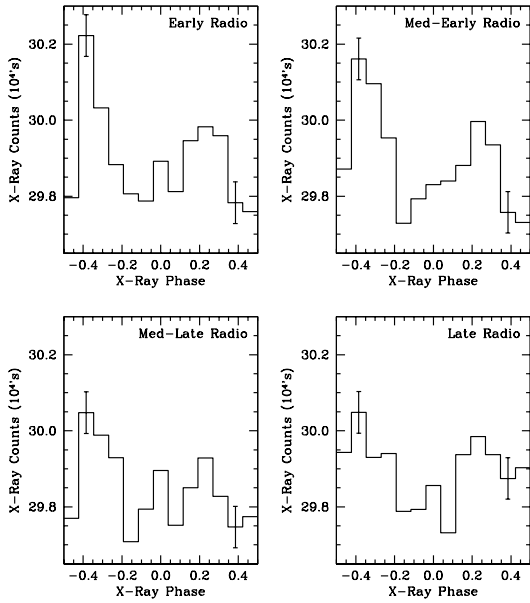


Fig. 2. Full-period X-ray profiles for photons detected during radio pulse arrival times falling in the four quartile bins shown in Figure 1. The radio peak falls at phase 0.5.

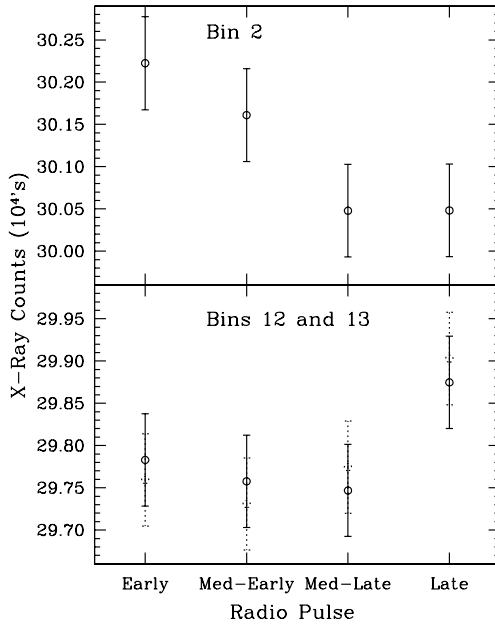


Fig. 4. The height of Bin 2, and of the dip in Bins 12 and 13, vs the lateness of the quartile.

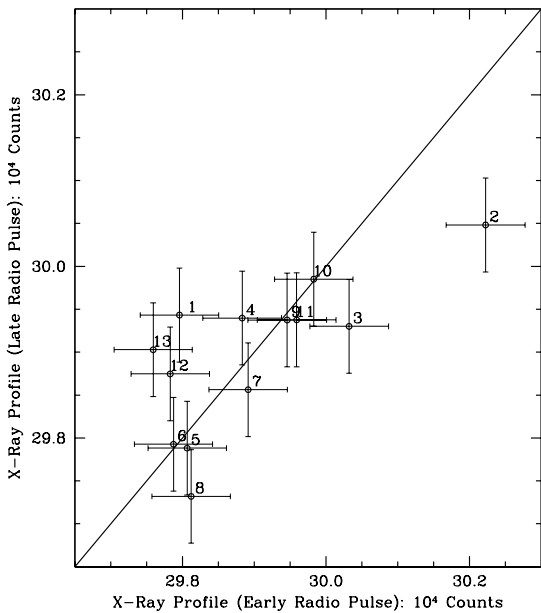


Fig. 3. Measured counts in the late radio phase quartile vs counts in the early radio phase quartile. X-ray phase bins are numbered sequentially beginning with 1.

a correlation but it cannot introduce it. Nonetheless, we used a number of techniques to ensure that our result was not produced by scintillation including subtracting

the average residual from each 5-minute span of data, and defining the four quartiles based on both 5-minute and 1-hour spans of data. More details can be found in Lommen et al.(2006). In summary, none of these techniques changed our results significantly.

5. Discussion

J01 showed that the giant micropulse emission occurs about 1 ms before the radio peak, so it is realistic to consider the possibility that the giant micropulse emission is primarily responsible for the early arrival of the radio pulse. The hypothesis is consistent with the timescale of the “early-ness”: the full-width at half-maximum of the histogram of arrival time residuals shown in Figure 1 is about 0.5 ms. However, the more detailed analysis performed in Lommen et al.(2006) shows that the effect cannot be explained by the occurrence of giant micropulses.

6. Theoretical Predictions

The results described above imply a connection between the radio and X-ray emission mechanisms for Vela that is not consistent with outer gap models. In these models, the high energy emission results from a gap connection to the pole opposite from that producing the radio emission. It is not clear how a correlation could exist between the radio and high energy regimes in these models. Petrova (2003, and references therein), however, offers a detailed model that could explain the correlation. She states that the non-thermal optical emission of rotation-powered pul-

sars should be considered as part of the broadband high-energy emission. Her models suggest that resonant absorption of radio emission from the outer magnetosphere leads to an increase in the pitch angles and momenta of the secondary pairs, which then leads to optical and higher energy emission by spontaneous synchrotron radiation.

7. Conclusions and Future Work

We have significant evidence linking features of Vela's X-ray emission with features of its radio emission. We find that X-ray pulses associated with early radio pulses show stronger emission at the main X-ray peak which is the sharper of the two. Similarly X-ray pulses associated with later radio pulses show stronger emission at the trough following the 2nd X-ray peak. We conclude that there is a close relationship between X-ray and radio emission in the Vela pulsar.

We plan to further characterize the relationship between the radio and high energy emissions of pulsars to identify their origins and constrain magnetospheric models. In particular, we will explore the dependence of radio-to-X-ray correlations on the radio frequency and polarization properties of individual Vela pulses, both of which carry information about emission altitudes. Similar observations of other pulsars also promise useful insights as probes of different magnetic field strengths and emission/viewing geometries.

Acknowledgements. Many thanks to Michael Kramer, Wim Hermsen, David Helfand and Paul Ray for helpful comments and to the Anton Pannekoek Institute at the University of Amsterdam for their hospitality, particularly Ben Stappers, Simone Migliari, Tiziana Di Salvo and Russell Edwards for useful discussions. JD and AL gratefully acknowledge the financial support of Franklin and Marshall College and a Research Corporation Grant in support of this work. ZA was supported by NASA grant NRA-99-01-LTSA-070. CRG acknowledges support of the National Science Foundation.

References

- Blackburn, J. K. 1995, In ASP Conf. Ser. 77: Astronomical Data Analysis Software and Systems IV, R. A. Shaw, H. E. Payne, and J. J. E. Hayes, eds., p. 367
- Cheng, K. S., Ruderman, M., & Zhang, L. 2000, *Astrophys. J.*, **537**, 964
- Cusumano, G., Hermsen, W., Kramer, M., Kuiper, L., Löhmer, O., Massaro, E., Mineo, T., Nicastro, L., & Stappers, B. W. 2003, *Astr. Astrophys.*, **410**, L9
- Daugherty, J. K., & Harding, A. K. 1996, *Astr. Astrophys. Supp.*, **120**, C107
- Harding, A. K., Strickman, M. S., Gwinn, C., Dodson, R., Moffet, D., & McCulloch, P. 2002, *Astrophys. J.*, **576**, 376
- Johnston, S., van Straten, W., Kramer, M., & Bailes, M. 2001, *Astrophys. J. Lett.*, **549**, L101
- Krishnamohan, S., & Downs, G. S. 1983, *Astrophys. J.*, **265**, 372

Lommen, A., Donovan, J., Gwinn, C., Arzoumanian, Z., Harding, A., Strickman, M., Dodson, R., McCulloch, P., & Moffett, D. 2006, *ApJ*, accepted

Petrova, S. A. 2003, *Mon. Not. R. Astr. Soc.*, **340**, 1229

Vivekanand, M. 2001, *Mon. Not. R. Astr. Soc.*, **326**, L33